

An automatic method for segmentation of fission tracks in epidote crystal photomicrographs

Alexandre Fioravante de Siqueira^a, Wagner Massayuki Nakasuga^a, Aylton Pagamisse^b, Carlos Alberto Tello Saenz^a, Aldo Eloizo Job^{a,*}

^a*DFQB - Departamento de Física, Química e Biologia
FCT - Faculdade de Ciências e Tecnologia
UNESP - Univ Estadual Paulista*

*Rua Roberto Simonsen, 305, 19060-900
Presidente Prudente, São Paulo, Brazil*

^b*DMC - Departamento de Matemática e Computação
FCT - Faculdade de Ciências e Tecnologia
UNESP - Univ Estadual Paulista*

*Rua Roberto Simonsen, 305, 19060-900
Presidente Prudente, São Paulo, Brazil*

Abstract

Manual identification of fission tracks has practical problems, such as variation due to observer-observation efficiency. An automatic processing method that could identify fission tracks in a photomicrograph could solve this problem and improve the speed of track counting. However, separation of non-trivial images is one of the most difficult tasks in image processing. Several commercial and free softwares are available, but these softwares are meant to be used in specific images. In this paper, an automatic method based on starlet wavelets is presented in order to separate fission tracks in mineral photomicrographs. Automatization is obtained by Matthews correlation coefficient, and results are evaluated by precision, recall and accuracy. This technique is an improvement of a method aimed at segmentation of scanning electron microscopy images. This method is applied in photomicrographs of epidote phenocrystals, in which accuracy higher than 89% was obtained in

*Corresponding author. Phones: +55(18)3229-5776 / +55(18)3229-5775.

Email addresses: siqueiraaf@gmail.com (Alexandre Fioravante de Siqueira), wamassa@gmail.com (Wagner Massayuki Nakasuga), aylton@fct.unesp.br (Aylton Pagamisse), tello@fct.unesp.br (Carlos Alberto Tello Saenz), job@fct.unesp.br (Aldo Eloizo Job)

Published in Computers & Geosciences (August 2014). The final publication is available at <http://dx.doi.org/10.1016/j.cageo.2014.04.008>.

fission track segmentation, even for difficult images. Algorithms corresponding to the proposed method are available for download. Using the method presented here, an user could easily determine fission tracks in photomicrographs of mineral samples.

Keywords: Epidote, Fission Track, Image Processing, Optical Microscopy, Wavelets

1. Introduction

Fission tracks are dislocated zones caused by nuclear fragments released in spontaneous fission of uranium-238. Information about fission tracks can be related to geologic events, as mineral crystallization age, geologic fault zones and thermal events[1].

Tracks crossing a polished mineral surface can be etched and visualized under an optical microscope, and its selection is based on the following relatively simple criteria[2, 3]:

- Fission tracks form straight line defects of a limited length ($< 20\mu m$);
- They exhibit no preferred orientation and disappear after suitable heating.

Manual identification of fission tracks has some practical problems, such as variation due to observer-observation efficiency. Also, Gleadow *et al.*[4] list some problems in discrimination of fission tracks from non-track defects as polishing scratches and resolving multiple track overlaps and small tracks amongst a similarly sized background of surface defects.

An automatic identification of fission track could solve this problem and improve the speed of track counting. Image processing can be used to automatize such task; however, separation of nontrivial images is one of the most difficult tasks in image processing[5]. Several commercial and free softwares are available for this purpose. Nonetheless, these softwares are meant to be used in specific images[6].

1.1. Proposed methodology

In this paper we propose an automatic method based on starlet wavelets, in order to segment fission tracks in images of natural minerals obtained by optical microscopy. Commonly used objective lenses (dry or oil immersion type) have total magnification up to 1500 times. In combination with a

reflected-transmitted light system, it is possible to analyze fission tracks[1, 7].

The proposed approach consists of applying starlet wavelets in a sample image to obtain its detail decomposition levels. Based on information retrieval (precision, recall and accuracy) and Matthews correlation coefficient (MCC), the segmentation level that better represents fission tracks of the original image is automatically chosen.

This technique is an improvement of a recent study aimed at segmentation of scanning electron microscopy images[8]. An application of this method is the separation of fission tracks in images of natural minerals, such as volcanic glasses, apatite, zircon, muscovite, epidote, among others.

In this paper, the proposed methodology is applied to segment fission tracks in photomicrographs of epidote crystals. Results presented in this study will be used as a basis to develop an open source software capable of extracting fission tracks from images of natural mineral samples in order to establish the age of the material using the fission track dating method[1]. A prototype of this software, containing the algorithms used in this study, is available for download on this journal website (see [Appendix A](#)).

The remainder of this paper follows. Section 2 introduces the material used in this study and starlet wavelets, as well as an overview of evaluation and automatization methods. Next, Section 3 presents the results from this method application in test photomicrographs. Moreover, the method performance is discussed. In the following, Section 4 presents the final considerations about this study. Finally, [Appendix A](#) explains where to obtain the cited algorithms and how to use them.

2. Material and Methods

2.1. Epidote crystals

Epidote is a mineral with monoclinic crystal structure and general formula $Ca_2(Al, Fe)_3Si_3O_{12}(OH)$ [9]. According to Poli and Schmidt[10], it is possible to have epidote formation at temperatures of $500 \sim 700^\circ C$ (pressure range of 0.2 to 0.6 GPa), and also at $720 \sim 760^\circ C$ (pressure range of 1.6 to 3 GPa). Their formation is given by different means. One of them is deuteric action, during the late phase of magmatic crystallization stage, by regional metamorphism and hydrothermal activity, *i.e.* percolation of solutions which chemically react with the rock through fractures, often in temperatures between 300 and $500^\circ C$ [11].

In order to evaluate the proposed methods, we used a data set consisting of 45 images. These images were obtained from epidote phenocrystals using a

Carl ZEISS optical microscope with Axiocam Imager.M1m system, nominal magnification factor of 1000X (dry) and transmitted light.

2.2. Starlet transform

Starlet wavelet transform is an isotropic redundant wavelet based on the algorithm “à trous” (with holes)[12, 13]. The construction of this wavelet is given by its scale and wavelet functions, respectively ϕ_{1D} and ψ_{1D} (Eqs. 1 and 2, [14, 15]), where ϕ_{1D} is the third order B-spline (B_3 -spline).

$$\phi_{1D}(t) = \frac{1}{12} (|t-2|^3 - 4|t-1|^3 + 6|t|^3 - 4|t+1|^3 + |t+2|^3) \quad (1)$$

$$\frac{1}{2}\psi_{1D}\left(\frac{t}{2}\right) = \phi(t) - \frac{1}{2}\phi\left(\frac{t}{2}\right) \quad (2)$$

An extension to two dimensions is achieved by a tensor product (Eq. 3),

$$\begin{aligned} \phi(t_1, t_2) &= \phi_{1D}(t_1)\phi_{1D}(t_2) \\ \frac{1}{4}\psi\left(\frac{t_1}{2}, \frac{t_2}{2}\right) &= \phi(t_1, t_2) - \frac{1}{4}\phi\left(\frac{t_1}{2}, \frac{t_2}{2}\right) \end{aligned} \quad (3)$$

These wavelets were successfully employed in analysis of astronomical [14, 15, 16] and biological [17] images, being suitable to evaluate images that contains isotropic objects. Isotropic transforms retrieve only one detail set per level instead of several detail sets (*e.g.* Daubechies wavelets have horizontal, vertical and diagonal detail levels), facilitating the interpretation of results. The properties of this wavelet (isotropy, redundancy, translation-invariance) make it a good alternative in image processing and pattern recognition.

Similarly to Eq. 3, the pair of filters (h, g) related to this wavelet is (Eq. 4, [15])

$$\begin{aligned} h_{1D}[k] &= [1 \ 4 \ 6 \ 4 \ 1]/16, k = -2, \dots, 2 \\ h[k, l] &= h_{1D}[k]h_{1D}[l] \\ g[k, l] &= \delta[k, l] - h[k, l] \end{aligned} \quad (4)$$

where δ is defined as $\delta[0, 0] = 1$, $\delta[k, l] = 0$ for $[k, l] \neq 0$. From Eqs. 3 and 4, detail wavelet coefficients are obtained from the difference between the current and previous resolutions.

Starlet transform application is given by a convolution between an input image c_0 and the finite impulse response (FIR) filter derived from ϕ (Eq. 5 [15]),

$$h = \begin{bmatrix} \frac{1}{256} & \frac{1}{64} & \frac{3}{128} & \frac{1}{64} & \frac{1}{256} \\ \frac{64}{3} & \frac{16}{3} & \frac{32}{9} & \frac{16}{3} & \frac{64}{3} \\ \frac{128}{1} & \frac{32}{1} & \frac{64}{3} & \frac{32}{1} & \frac{128}{1} \\ \frac{64}{1} & \frac{16}{1} & \frac{32}{3} & \frac{16}{1} & \frac{64}{1} \\ \frac{1}{256} & \frac{1}{64} & \frac{3}{128} & \frac{1}{64} & \frac{1}{256} \end{bmatrix} \quad (5)$$

This convolution results in a set of smoothing coefficients which correspond to the first decomposition level, c_1 . Detail wavelet coefficients of the first decomposition level are obtained from the difference $w_1 = c_0 - c_1$.

Let L be the last resolution level. Therefore, resolution levels can be calculated by:

$$\begin{aligned} c_j &= c_{j-1} * h, \\ w_j &= c_{j-1} - c_j, \end{aligned}$$

with $j = 0, \dots, L$, and $*$ the convolution operation. The set $W = \{w_1, \dots, w_L, c_L\}$ obtained by these operations is the starlet transform of the input image.

2.3. Evaluation of the results

In order to evaluate the proposed methodology, we employed precision, recall and accuracy[18, 19]. These values are based on the concepts of true positives (TP), true negatives (TN), false positives (FP) and false negatives (FN).

Fission tracks in an image sample are represented in a ground truth (GT) image: black represents the background, whereas white represents fission tracks in this image. Comparing an input image and its ground truth, TP, TN, FP and FN values could be established as:

- TP: pixels correctly labeled as fission tracks.
- FP: pixels incorrectly labeled as fission tracks.
- FN: pixels incorrectly labeled as background.
- TN: pixels correctly labeled as background.

Based on these considerations, precision (retrieved pixels that are relevant), recall (relevant pixels that were retrieved) and accuracy (proportion of true retrieved results) are defined:

$$\begin{aligned}
precision &= \frac{TP}{TP + FP} \\
recall &= \frac{TP}{TP + FN} \\
accuracy &= \frac{TP + TN}{TP + TN + FP + FN}
\end{aligned}$$

2.3.1. Method automatization

In order to establish the optimal level for method application, Matthews correlation coefficient (MCC, [20]) is used. MCC uses TP, TN, FP and FN, and may offer an evaluation of the segmentation correctness:

$$MCC = \frac{TP * TN - FP * FN}{\sqrt{(TP + FN)(TP + FP)(TN + FP)(TN + FN)}} \quad (6)$$

This coefficient measures how variables tend to have the same sign and magnitude, where 1, zero and -1 indicates perfect, random and imperfect predictions, respectively[21].

Thereby, automatic retrieval of the optimal segmentation level is achieved by:

- applying the method for L desired starlet decomposition levels;
- comparing method segmentation results with the image GT and obtaining TP, TN, FP and FN;
- calculating MCC (Eq. 6) for each L .

As the optimal segmentation level is reached, values yielded by MCC become higher. Then, the best segmentation level obtained by this method is the one that returns the highest MCC value.

2.4. Method overview

The proposed automatic segmentation method is defined as follows:

- Starlet transform is applied in an input image c_0 , resulting in L detail levels: D_1, \dots, D_L , where L is the last desired resolution level.

- First and second detail levels, D_1 and D_2 , are ignored due to the large amount of noise; third to i detail levels are summed ($R_i = D_3 + \dots + D_i$), where $3 \leq i \leq L$. This is the result of the method application related to starlet level i .
- TP, TN, FP and FN are obtained comparing R_i with its GT (see Section 2.3). MCC (Eq. 6) is calculated using these values.
- Therefore, the optimal segmentation level is the one that has a higher MCC between the R_L levels of method application.

To apply this method, one can use the pseudocodes given in Algorithm 1. Also, the source code of these algorithms in Matlab²/Octave³ programming language is available (see Appendix A).

Starlet transform of c_0 is given by $W = \{w_1, \dots, w_L, c_L\}$. `hgen()` (Algorithm 2), referenced on Algorithm 1, is applied when j is incremented. For $j > 1$, h has 2^{j-1} zeros between its elements, characterizing the *à trous* transform.

3. Experimental results

In order to present the proposed method results, six dataset images with different size and fission track distribution are shown (Fig. 1). The darker regions of these images correspond to fission tracks in epidote surface.

The proposed method was applied in the test images with $L = 3$ to $L = 9$. The optimal segmentation level was obtained from MCC, for each image. Also, precision, recall and accuracy were obtained for each level (Fig. 2), in order to evaluate the method performance. For a satisfactory segmentation degree, an optimal ratio between precision and recall becomes necessary.

One could see from Fig. 2 that accuracy and precision increases until level $L = 7$. On the other hand, recall decreases as L increases.

Fig. 1(a) will be used to introduce the proposed method. According to the first step, starlet transform detail levels are obtained from the input image (Fig. 3).

²Matlab is a numerical computing environment and a programming language developed by MathWorks. A trial version could be requested at <https://www.mathworks.com>.

³GNU Octave is an open source high-level interpreted language intended primarily for numerical computation. Download available freely at <http://www.gnu.org/software/octave/download.html>.

Algorithm 1: Pseudocode for automatic determination of fission tracks in an image, based on starlet algorithm application (adapted from [8, 16]).

Input:

- A grayscale image, c_0 .
- A ground truth image, gtc_0 .
- Number of resolutions to be calculated, L .

Output:

- Detail coefficients from starlet transform, w_j .
- An optimal image that presents fission tracks contained in the original image, $optft$.
- Matthews Correlation Coefficient (Eq. 6) between gtc_0 and the algorithm result for each level $imgft_i$, MCC_i , with $i = 3, \dots, L$.

```

1 mirroring( $c_0$ ); for  $j \leftarrow 1$  to  $L$  do
2    $h \leftarrow$  hgen( $j$ );
3    $c_j \leftarrow$  convolution( $c_{j-1}, h$ );
4    $w_j \leftarrow c_{j-1} - c_j$ ;
5   unmirroring( $c_j$ );
6   increment( $j$ );
7 initialize  $sum$  to 0;
8 for  $i \leftarrow 3$  to  $L$  do
9   for  $j \leftarrow 3$  to  $i$  do
10     $sum \leftarrow sum + w_j$ ;
11     $imgft_i \leftarrow sum$ ;
12     $MCC_i(imgft_i, gtc_0)$ ;
13  $optft \leftarrow \max(MCC_i)$ ;
14 return  $w_j, optft, MCC_i$ 

```

Algorithm 2: hgen: h filter generation and zero-inserting[8].

Input:

- h_{1D} filter, given by Eq. 4.
- Current resolution level, j .

Output:

- Filter h_{2D} , h .

```

1 if  $j = 0$  then
2   |  $h \leftarrow h_{1D}$ ;
3 else
4   |  $M \leftarrow \text{size}(h_{1D}, 2)$ ; initialize  $k$  to 0;
5   | for  $i \leftarrow 1$  step  $2^{i-1}$  to  $M + 2^{i-1} * (M - 1)$  do
6   |   | increment( $k$ );
7   |   |  $h(i) \leftarrow h_{1D}(k)$ ;
8 initialize  $aux$  to 0;
9  $aux \leftarrow \text{sum}(\text{sum}(h' * h))$ ;
10  $h \leftarrow (h' * h) / aux$ ;
11 return  $h$ 

```

After starlet application, Algorithm 1 is applied seven times, from $L = 3$ to $L = 9$. For example, method application for $L = 6$ consists of:

- disregard $D = 1$ (Fig. 3(a)) and $D = 2$ (Fig. 3(b)).
- sum $D = 3$ (Fig. 3(c)) to $D = 6$ (Fig. 3(f)): $\sum D_i, i = 3, \dots, 6$.

Results of the proposed method are shown as binary images, where fission tracks are represented by the white color and background by the black color (Fig. 4).

The next step is to determine the optimal segmentation level using MCC (Table 1). Values presented here are given in percentages in order to ease results comprehension. The optimal segmentation level for images of Fig. 1 is $L = 7$, according to MCC; then results obtained with $L = 7$ using the proposed method were compared to ground truth (GT).

GT images obtained from Fig. 1 are used to evaluate the method performance. These images were obtained manually by a specialist using GIMP⁴, an open source graphics software. TP pixels are shown as green, FN pixels

⁴Available freely at <http://www.gimp.org/downloads/>.

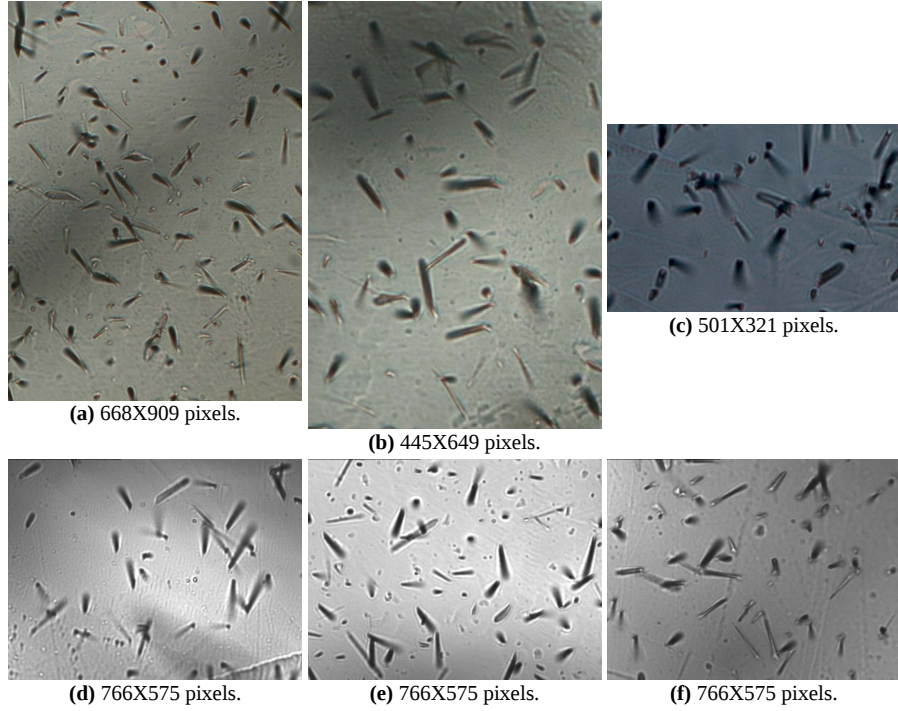


Figure 1: Photomicrographs of epidote phenocrystals. Fission tracks are shown in sample surface as dark segments. Nominal magnification factor: 1000X (dry).

as blue and FP pixels as red, to facilitate visualization of differences between the images (Fig. 5).

Most fission tracks presented in GT images were located using level $L = 7$. While precision and recall values vary, accuracy is higher than 89% for Fig. 1 images (Table 2). Comparing these results with near levels, $L = 6$ and $L = 8$, one can see that accuracy method for Fig. 1 using $L = 7$ is higher than with $L = 6$, but lower than $L = 8$ for Fig. 1(a),(d),(e) and (f). However, the difference is small for these cases, less than 1.5%. Furthermore, level 8 recall values are smaller than recall for $L = 7$ (difference between 14 and 22.5%).

Accurate results were obtained when images contained better visual state; for example, images without grain fractures (as seen in Fig. 1(d)). Also, textures in the background may lead to incorrect segmentation, thus lowering method accuracy. The red agglomerated regions in Fig. 4 exhibit this issue.

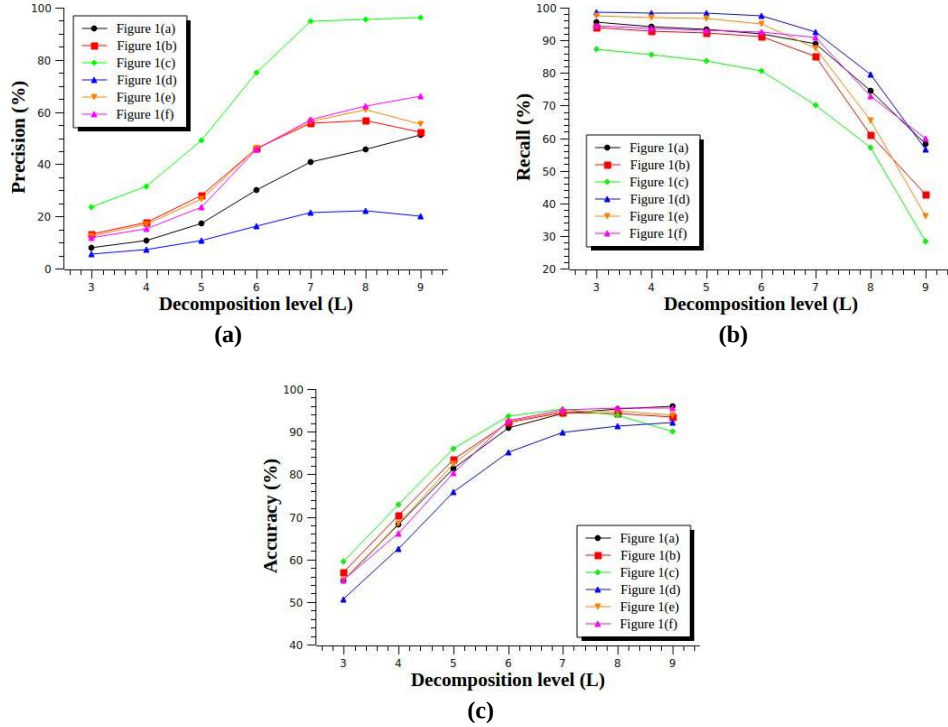


Figure 2: Precision, recall and accuracy values obtained from Fig. 1.

4. Conclusion

In this study we present a fission track automatic segmentation method for photomicrographs, based on starlet wavelets. This method uses starlet decomposition detail levels to determine edges of objects in an input image. Levels corresponding to noise are discarded and remain levels are summed. The method presented here can help the user to determine fission tracks in photomicrographs of mineral samples.

Automation is achieved using precision, recall and accuracy, together with Matthews correlation coefficient. MCC has proved to be a satisfactory measure to the method automation, representing a good balance between precision, recall and accuracy.

An application of this method is given here, in epidote crystal images obtained by optical microscopy. In this application, the proposed method presents a high accuracy degree, even for challenging images.

Algorithms used in this study are available for download. In future stud-

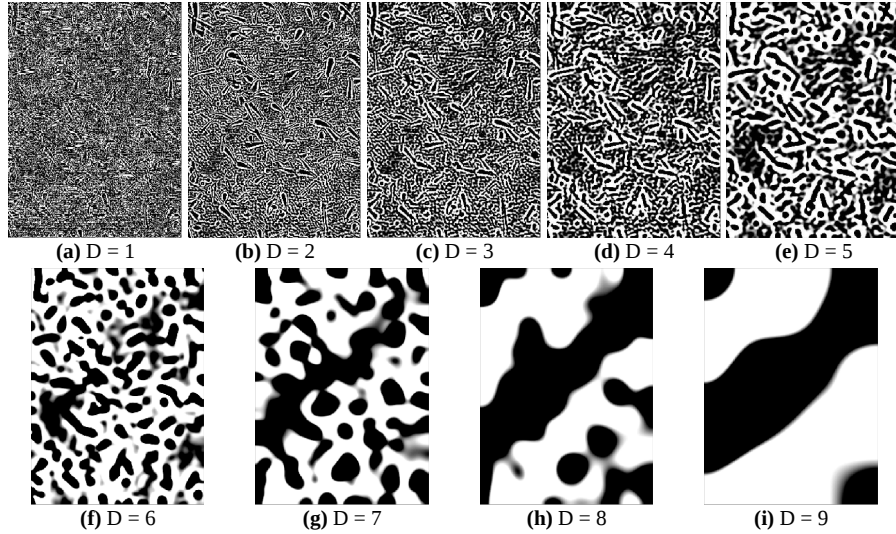


Figure 3: Starlet detail decomposition levels of Fig. 1(a). $D = 1$ and $D = 2$ were disregarded in method application due to noise amount. Although higher detail levels tend to aggregate, reducing segmentation accuracy, these levels present better information about fission tracks.

ies, this methodology will be used in images obtained by different materials, in order to estimate related features. Also, from this algorithms, an open source software aimed to analyze fission tracks in microscopical images will be built.

Acknowledgements

The authors would like to acknowledge the Brazilian foundations of research assistance CNPq, CAPES and FAPESP. This research is supported by FAPESP (Procs 2010/20496-2 and 2011/09438-3).

Appendix A. Supplementary material

To use the available supplementary algorithms, it is necessary to have two images: a sample image and its ground truth. These files could be put in the same folder of the algorithm files. In Matlab/Octave prompt, navigate to the folder that contains the algorithms. Then, type the following commands:

```
> IMG = imread('your_test_image');
> IMGGT = imread('your_ground_truth_image');
```

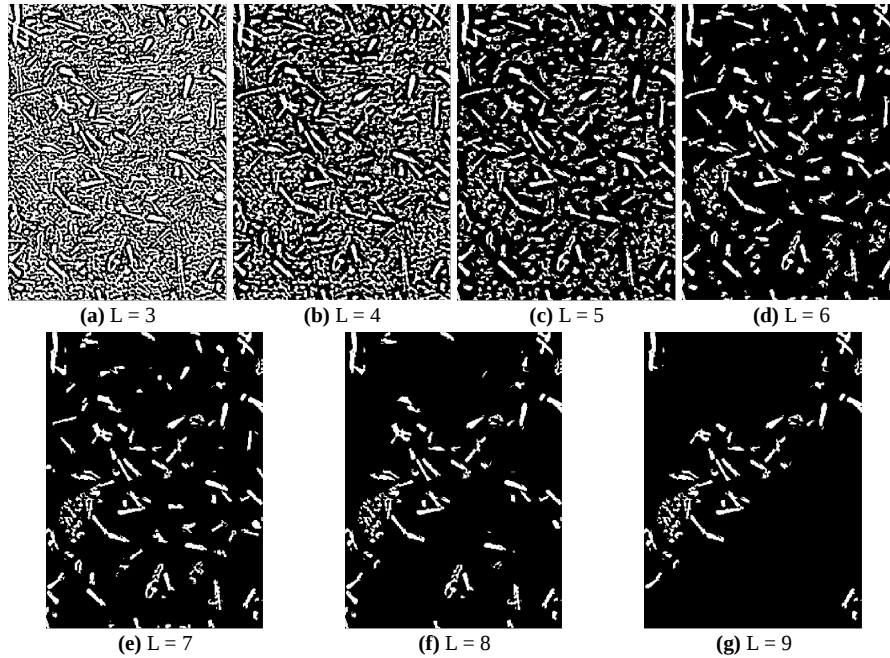


Figure 4: Segmentation output of the proposed method. Different levels, from $L = 3$ to $L = 9$ were considered.

```
> [D,L,COMP,MCC] = main(IMG,IMGTT);
```

where $>$ represents the Matlab/Octave prompt.

The software asks the desired application level, and returns starlet detail coefficients (D), the method output related to each starlet level (R), colored comparison between IMG and $IMGTT$ for each method level ($COMP$) and Matthews correlation coefficients also for each level (MCC). These files can be downloaded on this journal website.

References

- [1] G. Wagner, P. Van den Haute, Fission Track-Dating, Kluwer Academic Publishers, 1992.
- [2] R. Fleischer, P. Price, Techniques for geological dating of minerals by chemical etching of fission fragment tracks, *Geochimica et Cosmochimica Acta* 28 (1964) 1705–1714.
- [3] P. B. Price, Science and technology with nuclear tracks in solids, *Radiation Measurements* 40 (2005) 146–159.

Table 1: MCC obtained from method application for levels $L = 3$ to $L = 9$. $L = 7$ was the optimal segmentation level for Fig. 1 images, according to MCC values.

MCC (%)	L = 3	L = 4	L = 5	L = 6	L = 7	L = 8	L = 9
Fig. 1 (a)	19.32996	25.30251	35.37489	49.55525	57.85511	56.06013	52.62559
Fig. 1 (b)	24.22276	32.30995	45.43835	61.52304	66.14956	55.69191	43.78881
Fig. 1 (c)	29.07748	40.25502	56.84173	74.15157	79.22872	71.01649	49.15956
Fig. 1 (d)	16.09310	20.57131	27.80563	36.43833	41.70653	39.22664	30.58268
Fig. 1 (e)	24.60903	32.38622	45.38681	63.17591	67.75544	60.42723	41.72874
Fig. 1 (f)	22.82558	28.93141	40.72572	62.05960	69.84571	64.87040	60.59735

Table 2: Precision, recall and accuracy values for starlet application levels 6, 7 and 8.

	Precision (%)			Recall (%)			Accuracy(%)		
	L = 6	L = 7	L = 8	L = 6	L = 7	L = 8	L = 6	L = 7	L = 8
Fig. 1 (a)	30.047	40.674	45.556	91.918	88.860	74.529	90.899	94.232	95.306
Fig. 1 (b)	46.044	55.792	56.656	91.219	84.953	61.034	92.163	94.420	94.197
Fig. 1 (c)	74.977	94.820	95.545	80.685	70.104	56.958	93.731	95.428	93.805
Fig. 1 (d)	16.186	21.400	22.303	97.641	92.448	79.438	85.188	89.878	91.330
Fig. 1 (e)	46.118	56.291	60.873	95.075	87.678	65.457	92.369	94.711	94.960
Fig. 1 (f)	45.815	57.202	62.156	92.491	90.864	72.802	92.581	95.105	95.461

- [4] A. Gleadow, S. Gleadow, D. Belton, B. Kohn, M. Krochmal, R. Brown, Coincidence mapping - a key strategy for the automatic counting of fission tracks in natural minerals, Geological Society London: Special Publications 324 (2009) 25–36.
- [5] R. C. Gonzalez, R. E. Woods, Digital image processing, Prentice Hall, Upper Saddle River, N.J, 3rd ed edition, 2008.
- [6] M. Usaj, D. Torkar, M. Kanduser, D. Miklavcic, Cell counting tool parameters optimization approach for electroporation efficiency determination of attached cells in phase contrast images, Journal of Microscopy 241 (2011) 303–314.
- [7] A. Gleadow, I. Duddy, P. Green, J. Lovering, Confined fission track

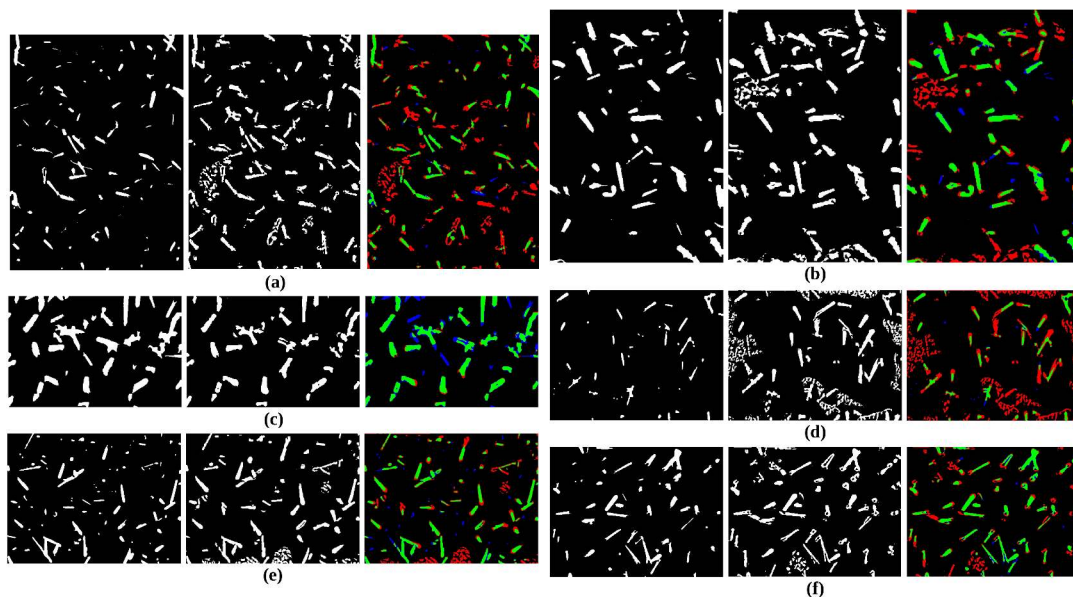


Figure 5: First column: Ground truths for Fig. 1 images. Second column: proposed method output for the optimal decomposition level. Third column: a comparison between GT and method output for optimal level (Green: TP pixels; blue: FN pixels; red: FP pixels).

lengths in apatite: a diagnostic tool for thermal history analysis, *Contributions to Mineralogy and Petrology* 94 (1986) 405–415.

- [8] A. F. de Siqueira, F. C. Cabrera, A. Pagamisse, A. E. Job, Segmentation of scanning electron microscopy images from natural rubber samples with gold nanoparticles using starlet wavelets, *Microscopy Research and Technique* 77 (2014) 71–78.
- [9] T. Ito, X-Ray studies on polymorphism, Maruzen Co. Ltd., Tokyo, 1950.
- [10] S. Poli, M. W. Schmidt, Experimental subsolidus studies on epidote minerals, *Reviews in Mineralogy and Geochemistry* 56 (2004) 171–195.
- [11] M. Bar, Y. Kolodny, Y. K. Bendor, Dating faults by fission track dating of epidotes: an attempt, *Earth and Planetary Science Letters* 22 (1974) 157–162.
- [12] M. Holschneider, R. Kronland-Martinet, J. Morlet, P. Tchamitchian, A real-time algorithm for signal analysis with the help of the wavelet

- transform, in: J.-M. Combes, A. Grossmann, P. Tchamitchian (Eds.), *Wavelets*, Springer Berlin Heidelberg, Berlin, Heidelberg, 1990, pp. 286–297.
- [13] M. Shensa, The discrete wavelet transform: wedding the a trous and mallat algorithms, *IEEE Transactions on Signal Processing* 40 (1992) 2464–2482.
- [14] J.-L. Starck, F. Murtagh, *Astronomical image and data analysis*, Springer, Berlin, 2006.
- [15] J.-L. Starck, F. Murtagh, J. Fadili, *Sparse image and signal processing: wavelets, curvelets, morphological diversity*, Cambridge University Press, Cambridge, New York, 2010.
- [16] J.-L. Starck, F. Murtagh, M. Bertero, Starlet transform in astronomical data processing, in: O. Scherzer (Ed.), *Handbook of Mathematical Methods in Imaging*, Springer New York, New York, NY, 2011, pp. 1489–1531.
- [17] A. Genovesio, J.-C. Olivo-Marin, Tracking fluorescent spots in biological video microscopy, *Proc. SPIE* 4964 (2003) 98–105.
- [18] D. L. Olson, D. Delen, *Advanced data mining techniques*, Springer, Berlin, 2008.
- [19] Q. Wang, Y. Yuan, P. Yan, X. Li, Saliency detection by multiple-instance learning, *Cybernetics, IEEE Transactions on* 43 (2013) 660–672.
- [20] B. W. Matthews, Comparison of the predicted and observed secondary structure of t4 phage lysozyme., *Biochimica et biophysica acta* 405 (1975) 442–451.
- [21] P. Baldi, S. Brunak, Y. Chauvin, C. A. F. Andersen, H. Nielsen, Assessing the accuracy of prediction algorithms for classification: an overview, *Bioinformatics* 16 (2000) 412–424.